Radiation effects on the electronic properties of bilayer graphene

Eric Suárez Morell[1] and Luis E. F. Foa Torres[2,*]

[1]*Departamento de Física, Universidad Técnica Federico Santa María, Casilla 110-V, Valparaíso, Chile*

[2]*Instituto de Física Enrique Gaviola (IFEG-CONICET) and FaMAF, Universidad Nacional de Córdoba, Ciudad Universitaria, 5000 Córdoba, Argentina*

(Received 6 June 2012; revised manuscript received 7 August 2012; published 28 September 2012)

We report on the effects of laser illumination on the electronic properties of bilayer graphene. By using Floquet theory combined with Green's functions, we unveil the appearance of laser-induced gaps not only at integer multiples of $\hbar\Omega/2$ but also at the Dirac point with features which are shown to depend strongly on the laser polarization. Trigonal warping corrections are shown to lead to important corrections for radiation in the terahertz range, reducing the size of the dynamical gaps. Furthermore, our analysis of the topological properties at low energies reveals that, when irradiated with linearly polarized light, ideal bilayer graphene behaves as a trivial insulator, whereas circular polarization leads to a nontrivial insulator per valley.

DOI: 10.1103/PhysRevB.86.125449 PACS number(s): 72.80.Vp, 03.65.Vf, 72.10.−d

I. INTRODUCTION

Among the many promises sparked by graphene research during the last few years,[1,2] graphene optoelectronics is perhaps one of the brightest.[3–6] From improved power conversion of energy harvesting devices[7] to novel plasmonics properties,[8,9] graphene and related materials offer an outstanding playground for the study of light-matter interaction, with many potential applications.[3,4,10,11]

Recent studies pointed out the intriguing possibility of inducing band gaps in monolayer graphene by illumination with a laser field.[12–14] The peculiar electronic structure of graphene and its low dimensionality are crucial for the occurrence of this effect. Further studies have predicted observable changes in the conductance[15,16] and optical properties,[17] with a strong dependence on laser polarization,[15,18] motivating many other interesting studies.[19–23] Moreover, the possibility of controlling topological insulators with photocurrents,[11] as well as the emergence of nontrivial laser-induced topological properties and edge states,[16,19,24,25] the so-called Floquet topological insulators, adds more relevance to this area.

Graphene's thicker cousin, bilayer graphene (BLG), has also shown enormous potential,[1,2] allowing for a tunable band gap[29] as required for the operation of active devices. However, the studies mentioned in the previous paragraph were all centered on monolayer graphene. Only in Ref. 30 did the authors propose an irradiated bilayer as a vehicle for inducing a valley polarized current. Here, we focus on the electronic and topological properties of BLG illuminated by a laser with a frequency either in the terahertz or in the midinfrared range. In the terahertz range, trigonal warping (TW) corrections are shown to induce strong modifications in the theoretical predictions, leading to, besides qualitative changes in the spectra, quantitative differences in the laser-induced gaps up to a factor of 2.

Moreover, we show that a laser field may also lead to polarization-tunable topological properties in BLG ranging from a trivial insulator to one with properties akin to those of a topological insulator. Specifically, we show that the low-energy properties of BLG illuminated by circularly polarized light can be described by a simple effective Hamiltonian similar to the one for BLG with a bias. Our theoretical analysis shows that although the system behaves as a trivial insulator in the presence of linearly polarized light, switching the polarization to circular transforms it into a nontrivial insulator per valley.

II. RESULTS AND DISCUSSION

A. Floquet theory applied to irradiated bilayer graphene

The unit cell of BLG with Bernal stacking has two inequivalent sites, labeled $A1$ and $B1$ on the top layer and $A2$ and $B2$ on the bottom layer; they are arranged in such a way that atom $B1$ lies on top of atom $A2$. Using the wave functions $\Psi = (\psi_{A1}, \psi_{B2}, \psi_{A2}, \psi_{B1})^T$ for the K valley and $\Psi = (\psi_{B2}, \psi_{A1}, \psi_{B1}, \psi_{A2})^T$ for the K' valley, an effective Hamiltonian for the low-energy properties is given by[31]

$$H_0(\vec{k}) = \xi \begin{pmatrix} 0 & v_3\pi & 0 & v\pi^\dagger \\ v_3\pi^\dagger & 0 & v\pi & 0 \\ 0 & v\pi^\dagger & 0 & \xi\gamma_1 \\ v\pi & 0 & \xi\gamma_1 & 0 \end{pmatrix}, \tag{1}$$

where $\xi = 1(-1)$ for valley $K(K')$, $\pi = p_x + i\ p_y$, $v = (\sqrt{3}/2)a\gamma_0/\hbar$, $v_3 = (\sqrt{3}/2)a\gamma_3/\hbar$, $a = 0.246$ nm, graphene lattice constant, $\gamma_0 = 3.16$ eV, $\gamma_1 = 0.39$ eV, and $\gamma_3 = 0.315$ eV. The hopping parameter γ_3 is responsible for the TW effects.

We apply linearly or circularly polarized light perpendicular to the graphene bilayer as shown schematically in Fig. 1(a). The time-dependent field is introduced through the substitution $\vec{k} \to \vec{k} + e\vec{A}/\hbar$, where the vector potential is $\vec{A}(t) = A(\cos(\Omega t), \cos(\Omega t + \phi))$, where $\phi = 0(\pi/2)$ for linear(circular) polarization. The Floquet theorem[32–34] provides an elegant route to handle this time-periodic Hamiltonian $[H(t+T) = H(t) = H_0(\vec{k} + e\vec{A}(t)/\hbar)$, where $T = 2\pi/\Omega]$, it states that the solutions to the time-dependent Schrödinger equation can be written as $\Psi_\alpha(\vec{r},t) = e^{-i\varepsilon_\alpha t/\hbar}\phi_\alpha(\vec{r},t)$, where $\phi_\alpha(t) = \phi_\alpha(t+T)$ is time periodic, the Floquet states can be further expanded into a Fourier series, $\phi_\alpha(t) = \sum e^{in\Omega t}\phi_\alpha^{(n)}$, and a substitution in the Schrödinger equation gives

$$\sum_m (H^{(n,m)} - n\hbar\Omega\delta_{n,m}) \left|\phi_\alpha^{(n)}\right\rangle = \epsilon_\alpha \left|\phi^{(n)}\right\rangle, \tag{2}$$

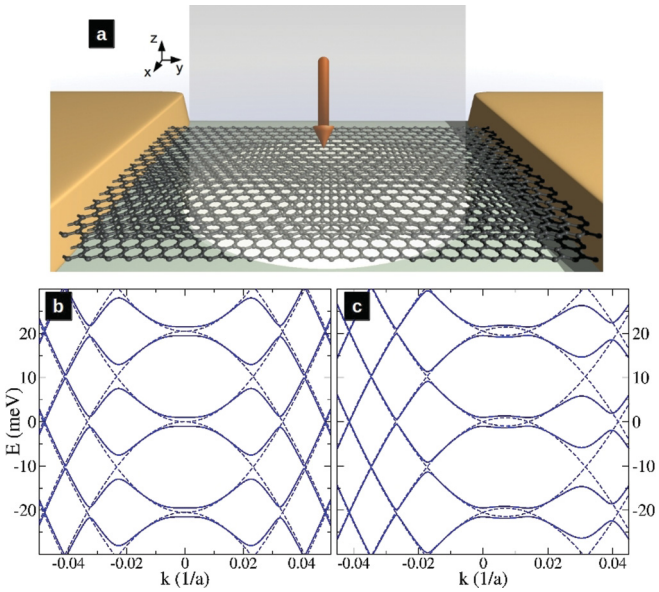

FIG. 1. (Color online) (a) Scheme of the considered setup where a laser field is applied perpendicular to a graphene bilayer. (b, c) Quasienergy Floquet band structure for a bulk bilayer (b) without and (c) with trigonal warping. These plots are along the k_x direction ($k_y = 0$); solid lines are for circularly polarized light with a frequency of 5 THz and an intensity of 0.5 mW/μm^2. The unirradiated spectrum is shown by dashed lines.

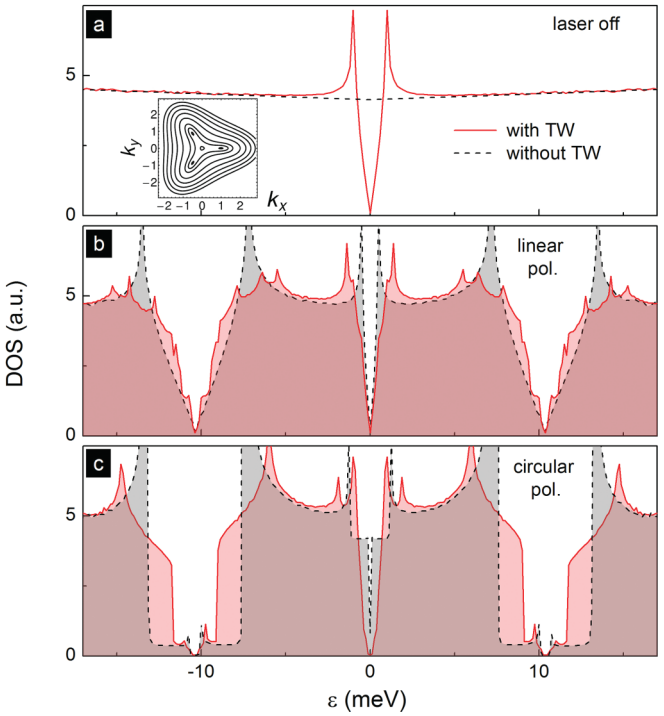

FIG. 2. (Color online) (a) DOS for bilayer graphene with the laser turned off. The solid line corresponds to calculations performed including trigonal warping (TW) corrections; the dashed line, to calculations without them. Inset: Isoenergy lines for the dispersion of bilayer graphene in the absence of radiation; strong TW distortion is evident. (b, c) DOS as defined in the text for bilayer graphene in the presence of linearly (b) and circularly (c) polarized light (5 THz) with an intensity of 0.5 mW/μm^2.

where $H^{(n,m)} = \frac{1}{T}\int_0^T dt\, H(t) e^{i(n-m)\Omega t}$ and ϵ_α is the so-called quasienergy. Simple inspection shows that this is an eigenvalue equation analogous to the one for time-independent systems. There are, however, two main differences: the role of the Hamiltonian is played by the so-called Floquet Hamiltonian, $H_F = H - i\hbar\, d/dt$; and the states belong to an extended Hilbert space which is the direct product between the usual Hilbert space and the space of time-periodic functions with period T. It is straightforward to see that $H_F^{(n,m)} = H^{(n,m)} - n\hbar\Omega\delta_{n,m}$. This method has been applied to a variety of systems and, in particular, to ac fields such as alternating gate voltages in graphene[35,36] beyond the adiabatic limit.

The time-averaged density of states (DOS) gives valuable information on the Floquet spectra in a compact form and can be calculated as in Refs. 13 and 15. To this end we compute the Floquet-Green function, defined as $\mathbf{G}_F = (\varepsilon\mathbf{1} - \mathbf{H}_F)^{-1}$, from which the time-averaged DOS is obtained as $\mathrm{DOS}(\varepsilon) = -\frac{1}{\pi}\mathrm{Im}\{\mathrm{Tr}(\mathbf{G}_F(\varepsilon))_{0,0}\}$, where $(\mathbf{G}_F)_{0,0}$ stands for the sub-block of the Floquet-Green function corresponding to the vanishing Fourier index.

B. Laser-induced modifications of the Floquet spectra

In the following we analyze the behavior of the quasienergy spectra and the DOS for various laser intensities, frequencies, and polarization.[37] While in monolayer graphene, TW introduces small corrections which become noticeable only at high energies (∼500 meV), in the case of BLG these corrections are stronger at low energies, where they lead to a splitting of the Dirac point into a structure with four pockets[31] as shown in the inset in Fig. 2(a). Here we show that these effects, which were neglected in previous studies of irradiated bilayer, are indeed very important for radiation in the terahertz range.

Figure 1 shows the quasienergy dispersion along a particular k direction without [Fig. 1(b)] and with [Fig. 1(c)] the TW correction in the presence of the electromagnetic field. The dashed lines in each figure show the unirradiated case. The field is expected to have a stronger effect at the crossing points, which, due to the electron-hole symmetry, are located at integer multiples of $\hbar\Omega/2$ above and below the Dirac point, as shown in Figs. 1(b) and 1(c). The time-dependent perturbation introduces a nonvanishing matrix element between the states at those crossings, thereby lifting the degeneracies and opening the so-called dynamical gaps.[12,13] The gap at the charge neutrality point is a higher order effect and is analyzed in more detail later.

Figure 2 shows the DOS for BLG in the presence of either linearly [Fig. 2(b)] or circularly [Fig. 2(c)] polarized light (5 THz), with (solid line) and without (dashed line) TW. The DOS in the absence of radiation is shown in Fig. 2(a) for reference. Although from the preceding discussion, one might expect the main corrections to arise only close to the Dirac point, Figs. 2(b) and 2(c) show that they emerge even at the dynamical gaps for radiation in the terahertz range.

For linearly polarized light, the DOS in the vicinity of $\hbar\Omega/2$ exhibits a depletion area with a linear dispersion and a single point of vanishing DOS. This is similar to the case of monolayer graphene found in Ref. 15 and is due to the fact

that the gap depends on the relative angle between k and the polarization vector; no gap emerges when they are parallel. One can also note that the roughly linear dispersion around the dynamical gaps acquires a structure with three narrow features on each side when TW corrections are included. This is a consequence of the deformation of the isoenergy lines in the k_x-k_y plane due to the TW corrections [see inset in Fig. 2(a)].

For circular polarization, two striking observations not reported before should be emphasized: (i) there is a gap opening at zero energy [which also occurs in the absence of TW but is much smaller and cannot be distinguished in the figure; see inset in Fig. 1(b)]; and (ii) the dynamical gap (which turns out to be linear in the field intensity as for monolayer graphene) is overestimated by a factor of almost 2 when TW corrections are not taken into account. A key factor behind these differences is, again, the breaking of the rotational symmetry in the k_x-k_y plane even for low energies. Although the gap at the charge neutrality point would require stringent conditions (being about 0.3 meV for a laser intensity of 0.5 mW/μm^2), the physics described here may prompt additional research and experiments that may allow directly or indirectly unveiling it. In contrast, the effects described at the dynamical gaps ($\pm\hbar\Omega/2$) are much stronger and should be observable in low-temperature experiments. Indeed the dynamical gaps are of the order of 5 K for 10-THz radiation at 0.5 mW/μm^2 and reach larger values (up to 30 meV, or 350 K) for 30-THz radiation for a power of a few mW/μm^2.

As one moves to higher frequencies, TW effects become less noticeable, though the depletion areas may become larger and therefore easier to observe experimentally. Figure 3 highlights this for three frequencies—5 THz [Fig. 3(a)], 10 THz [Fig. 3(b)], and 30 THz [which corresponds to the midinfrared range; Fig. 3(c)]—for linearly (dashed line) and circularly (solid line) polarized light.

C. Effective low-energy Hamiltonian description and topological considerations

Though more academic in nature, we now turn to an instructive analysis of the low-energy and topological properties of irradiated BLG. Our main fundamental question is, Are nontrivial laser-induced topological states to be expected in BLG? To this end, we are interested in obtaining an effective Hamiltonian to describe low-energy electronic properties for low values of the light intensity in the spirit of Kitagawa and coworkers.[25] We consider only the process when one photon is absorbed (emitted) and then re-emitted (reabsorbed), in this case applying the continued fraction method and retaining only the terms of order $O(F^2)$, where $F = eA/\hbar$ and, in the following, $\hbar = 1$, the effective time-independent Hamiltonian can be expressed as

$$H_{\rm eff} = H_0 + V_{-1}\hat{G}(-1,\Omega)V_{+1} + V_{+1}\hat{G}(+1,\Omega)V_{-1}, \quad (3)$$

where $V_{\pm 1} = H^{(n,m)}$ for $n - m = \pm 1$ and $\hat{G}(n,\Omega) = \frac{1}{\epsilon + n\Omega - H_0}$ represents the propagator of a particle with n photons. For circularly polarized light, this results in the effective

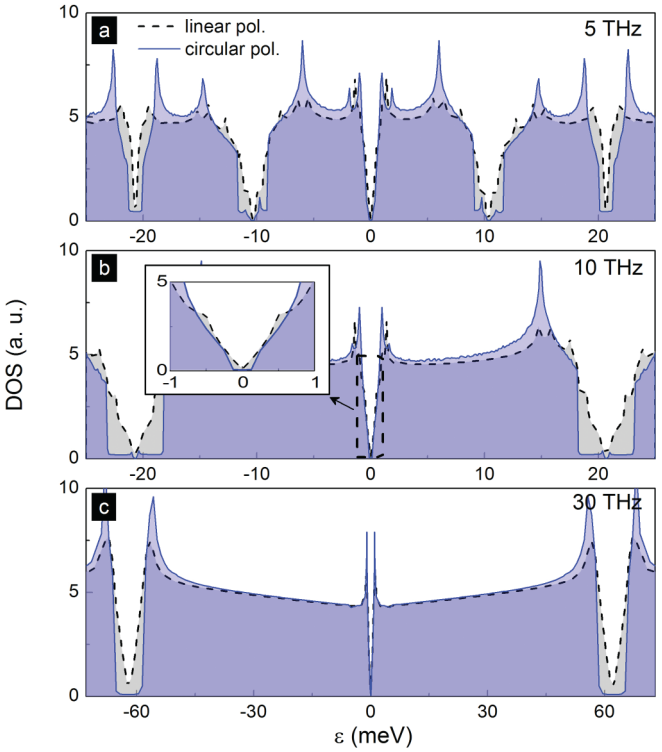

FIG. 3. (Color online) DOS as a function of energy for (a) 5 THz, (b) 10 THz, and (c) midinfrared 30-THz radiation. (a, b) Computed for a laser intensity of 0.5 mW/μm^2; (c) computed for 10 mW/μm^2. Solid (dashed) lines are for circular (linear) polarization. Note the change in the horizontal scale in (c). The structure induced by TW becomes smoothed as the frequency increases. Inset in (b): A zoom around zero energy.

Hamiltonian

$$H = \xi \begin{pmatrix} \frac{F^2 v_3^2}{\Omega} + \frac{F^2 v^2 \Omega}{\gamma_1^2} & v_3\pi & 0 & v\pi^\dagger \\ v_3\pi^\dagger & -\frac{F^2 v_3^2}{\Omega} - \frac{F^2 v^2 \Omega}{\gamma_1^2} & v\pi & 0 \\ 0 & v\pi^\dagger & -\frac{F^2 v^2}{\Omega} & \xi\gamma_1 \\ v\pi & 0 & \xi\gamma_1 & \frac{F^2 v^2}{\Omega} \end{pmatrix}, \quad (4)$$

where we have assumed $\gamma_1 \gg \Omega \gg \epsilon$. All terms on the diagonal should be multiplied by a factor $\eta = \pm 1$ to take into account left or right polarization of the light. Strikingly, this effective Hamiltonian resembles the Hamiltonian of BLG with a bias, but a careful analysis reveals some subtle differences. One may argue that laser illumination introduces three ingredients: First, it breaks the intralayer symmetry by introducing a term similar to the Kane-Mele spin-orbit term (F^2v^2/Ω)[25,26] (if the layers were decoupled, the system would have a gap solely due to this term); second, it breaks the inversion symmetry between the two layers (similar to a potential difference between layers), an effect which also opens a gap; and third, when a graphene-based system with a gap is exposed to circularly polarized light, an asymmetry between the valleys is expected due to the breaking of inversion symmetry, an effect similar to optical circular dichroism for valleys instead of spins.[27,28] The valley degree of freedom can be exploited, generating valley-dependent currents as we argue below.

The gap at $k = 0$ is given by $2 \times (\frac{F^2 v_3^2}{\Omega} + \frac{F^2 v^2 \Omega}{\gamma_1^2})$, and the relative importance of these two terms is set by the frequency Ω: for Ω in the terahertz range the TW term has a leading impact on the gap as noted in the discussion of Fig. 2.

To evaluate the topological properties of this effective Hamiltonian we reduce the previous 4×4 to a 2×2 Hamiltonian which describes the effective interaction between the nondimer sites A1 and B2. Considering, as before, $\gamma_1 \gg \epsilon$ the new effective low-energy Hamiltonian is given by

$$H = \varepsilon_0 \begin{pmatrix} \Delta & k_{-\xi}^2 - s\xi k_\xi \\ k_\xi^2 - s\xi k_{-\xi} & -\Delta \end{pmatrix}, \qquad (5)$$

where $\varepsilon_0 = (\gamma_3/\gamma_0)^2 \gamma_1 \approx 4$ meV, $\Delta = \eta F'^2 (\frac{1}{\Omega'} + \frac{\gamma_3^2 \Omega'}{\gamma_0^2})$, $\xi = 1(-1)$ for valley $K(K')$, $k_\pm = (k_x \pm i k_y)/k_0$, $k_0 = 2\gamma_3\gamma_1/(\sqrt{3} a \gamma_0^2)$, $a = 0.246$ nm, and F' and Ω' are now dimensionless parameters given in k_0 and ε_0 units, respectively. The parameter s takes values of (1,0) including or not including the TW. For values of $\Omega \ll \gamma_1$ the second term in the expression of Δ can be neglected and it gives a quite simple dependence of the gap on F' and Ω', Gap $= 2 \times \varepsilon_0 \frac{F'^2}{\Omega'}$. This expression shows an excellent agreement with numerical calculations in the frequency range considered to obtain Eq. (4).

From this effective Hamiltonian it is straightforward to calculate the Berry curvature and the Chern number.[38] The curvature is given in polar coordinates by

$$\Omega(k,\theta) = \frac{\xi \eta \Delta (4k^2 - s^2)}{2(\Delta^2 + k^4 + k^2 s^2 - 2k^3 \xi s \cos 3\theta)^{3/2}}, \qquad (6)$$

and the integration gives an integer nonzero Chern number per valley, a quantum valley-Hall state.[39] The Chern number has opposite values for the two valleys for a given handedness of polarization. A valley current will be proportional to the Berry curvature.[40] Therefore a change in the handedness implies a change in the direction of the valley currents, as the sign of the Berry curvature changes. It provides an effective way to control these valley currents. There have been some proposals regarding this subject; see, for instance, Refs. 41 and 42. On the other hand, the structure of the Berry curvature reveals the impact of TW: For low values of Δ the shape of the curvature shows a central dip with a topological charge $Q = -1$ and three peaks, away from the center and separated 120°, with $Q = 1$ each; in the K' valley we have the opposite behavior. This segregation might have an impact on the edge currents of a system based on BLG and energies in the terahertz range.[43]

A completely different picture is obtained from irradiating BLG with linearly polarized light. Following the same procedure as before, one obtains a gap at $k = 0$, with a peculiar behavior; it does not depend explicitly on Ω or on γ_3, Gap $= 2 \times \frac{F^2 v^2}{\gamma_1}$. The Chern number equals 0 in every valley, thus the states are topologically trivial.

III. CONCLUSIONS

In summary, the effects of a laser with frequencies ranging from terahertz to the midinfrared on the electronic structure of BLG are analyzed, highlighting the appearance of laser-induced gaps and their dependence on the light polarization as well as the strong influence of TW corrections. For radiation in the terahertz range, TW in BLG tends to decrease the size of the dynamical gaps at $\pm\hbar\Omega/2$; this is very different from the case of monolayer graphene, where TW effects are much weaker.[15] Furthermore, we obtain a time-independent effective Hamiltonian which serves as a starting point for the determination of the topological properties of the associated low-energy states. We find that while, for both polarizations, there is a small gap at zero energy, their topological origin is different: The Chern number in the presence of linearly polarized light equals 0, a trivial insulator, while it is a nonzero integer, a quantum valley-Hall insulator, when the light is circularly polarized. Though more difficult to observe experimentally than dynamical gaps, further work in this direction may open promising prospects for exploiting the valley degree of freedom in graphene-based structures.

ACKNOWLEDGMENTS

We acknowledge discussions with D. Soriano Hernandez and H. L. Calvo. E.S.M. acknowledges support from DGIP and UTFSM. L.E.F.F.T. acknowledges funding from SeCyT-UNC, SPU Mercosur (PPCP 0025-2011) and ANPCyT-FonCyT and support from the Alexander von Humboldt Foundation and the ICTP of Trieste.

*Corresponding author: lfoa@famaf.unc.edu.ar

[1] A. K. Geim, Science **324**, 1934 (2009); A. K. Geim and K. S. Novoselov, Nat. Mat. **6**, 183 (2007).

[2] A. H. Castro Neto, F. Guinea, N. M. R. Peres, K. S. Novoselov, and A. K. Geim, Rev. Mod. Phys. **81**, 109 (2009); N. M. R. Peres, *ibid.* **82**, 2673 (2010).

[3] F. Bonaccorso, Z. Sun, T. Hasan, and A. C. Ferrari, Nat. Phot. **4**, 611 (2010).

[4] F. Xia, Th. Mueller, Y.-m. Lin, A. Valdes-Garcia, and Ph. Avouris, Nat. Nanotech. **4**, 839 (2009).

[5] J. Karch, C. Drexler, P. Olbrich, M. Fehrenbacher, M. Hirmer, M. M. Glazov, S. A. Tarasenko, E. L. Ivchenko, B. Birkner, J. Eroms, D. Weiss, R. Yakimova, S. Lara-Avila, S. Kubatkin, M. Ostler, T. Seyller, and S. D. Ganichev, Phys. Rev. Lett. **107**, 276601 (2011).

[6] G. Konstantatos, M. Badioli, L. Gaudreau, J. Osmond, M. Bernechea, F. Pelayo Garcia de Arquer, F. Gatti, and F. H. L. Koppens, Nat. Nanotech. **7**, 363 (2012).

[7] N. M. Gabor, J. C. W. Song, Q. Ma, N. L. Nair, T. Taychatanapat, K. Watanabe, T. Taniguchi, L. S. Levitov, and P. Jarillo-Herrero, Science **334**, 6056 (2011).

[8] F. H. L. Koppens, D. E. Chang, and F. Javier Garcia de Abajo, Nano Lett. **11**, 3370 (2011).

[9] J. Chen, M. Badioli, P. Alonso-Gonzalez, S. Thongrattanasiri, F. Huth, J. Osmond, M. Spasenovic, A. Centeno, A. Pesquera, Ph. Godignon, A. Zurutuza Elorza, N. Camara, F. J. Garcia de Abajo, R. Hillenbrand, and F. H. L. Koppens, Nature **487**, 77 (2012).

[10] L. Ren, C. L. Pint, L. G. Booshehri, W. D. Rice, X. Wang, D. J. Hilton, K. Takeya, I. Kawayama, M. Tonouchi, R. H. Hauge, and J. Kono, Nano Lett. **9**, 2610 (2009).

[11]J. W. McIver, D. Hsieh, H. Steinberg, P. Jarillo-Herrero, and N. Gedik, Nat. Nanotech. **7**, 96 (2012).
[12]S. V. Syzranov, M. V. Fistul, and K. B. Efetov, Phys. Rev. B **78**, 045407 (2008); F. J. Lopez-Rodriguez and G. G. Naumis, *ibid*. **78**, 201406(R) (2008).
[13]T. Oka and H. Aoki, Phys. Rev. B **79**, 081406(R) (2009).
[14]O. V. Kibis, Phys. Rev. B **81**, 165433 (2010).
[15]H. L. Calvo, H. M. Pastawski, S. Roche, and L. E. F. Foa Torres, Appl. Phys. Lett. **98**, 232103 (2011).
[16]Z. Gu, H. A. Fertig, D. P. Arovas, and A. Auerbach, Phys. Rev. Lett. **107**, 216601 (2011).
[17]Y. Zhou and M. W. Wu, Phys. Rev. B **83**, 245436 (2011).
[18]S. E. Savelev and A. S. Alexandrov, Phys. Rev. B **84**, 035428 (2011).
[19]B. Dóra, J. Cayssol, F. Simon, and R. Moessner, Phys. Rev. Lett. **108**, 056602 (2012).
[20]A. Iurov, G. Gumbs, O. Roslyak, and D. Huang, J. Phys.: Condens. Matter **24**, 015303 (2012).
[21]J. Liu, F.-H. Su, H. Wang, and X. Deng, New J. Phys. **14**, 013012 (2012).
[22]M. Busl, G. Platero, and A.-P. Jauho, Phys. Rev. B **85**, 155449 (2012).
[23]P. San-Jose, E. Prada, H. Schomerus, and S. Kohler, arXiv:1206.4411 [cond-mat.mes-hall].
[24]N. H. Lindner, G. Refael, and V. Galitski, Nature Phys. **7**, 490 (2011).
[25]T. Kitagawa, T. Oka, A. Brataas, L. Fu, and E. Demler, Phys. Rev. B **84**, 235108 (2011); T. Kitagawa, E. Berg, M. Rudner, and E. Demler, *ibid*. **82**, 235114 (2010).
[26]C. L. Kane and E. J. Mele, Phys. Rev. Lett. **95**, 226801 (2005).
[27]W. Yao, D. Xiao, and Q. Niu, Phys. Rev. B **77**, 235406 (2008).
[28]J.-i. Inoue, Phys. Rev. B **83**, 205404 (2011).
[29]Y. Zhang, T.-T. Tang, C. Girit, Z. Hao, M. C. Martin, A. Zettl, M. F. Crommie, Y. R. Shen, and F. Wang, Nature **459**, 820 (2009).
[30]D. S. L. Abergel and T. Chakraborty, Appl. Phys. Lett. **95**, 062107 (2009); Nanotechnology **22**, 015203 (2011).
[31]E. McCann and V. I. Falko, Phys. Rev. Lett. **96**, 086805 (2006); E. McCann, D. S. L. Abergel, and V. I. Falko, Solid State Commun. **143**, 110 (2007).
[32]G. Platero and R. Aguado, Phys. Rep. **395**, 1 (2004).
[33]S. Kohler, J. Lehmann, and P. Hänggi, Phys. Rep. **406**, 379 (2005).
[34]L. E. F. Foa Torres, Phys. Rev. B **72**, 245339 (2005).
[35]L. E. F. Foa Torres, H. L. Calvo, C. G. Rocha, and G. Cuniberti, Appl. Phys. Lett. **99**, 092102 (2011).
[36]P. San-Jose, E. Prada, S. Kohler, and H. Schomerus, Phys. Rev. B **84**, 155408 (2011).
[37]The photothermal response of the system is not considered here. In an actual experiment further measurements of their different polarization and wavelength dependences may help to distinguish them.
[38]D. Xiao, M.-C. Chang, and Q. Niu, Rev. Mod. Phys. **82**, 1959 (2010).
[39]A numerical calculation of the Chern number based on the 4×4 Hamiltonian gives the same result.
[40]M.-C. Chang and Q. Niu, Phys. Rev. Lett. **75**, 1348 (1995).
[41]H. Schomerus, Phys. Rev. B **82**, 165409 (2010).
[42]I. Martin, Ya. M. Blanter, and A. F. Morpurgo, Phys. Rev. Lett. **100**, 036804 (2008).
[43]A. S. Núñez, E. Suárez Morell, and P. Vargas, Appl. Phys. Lett. **98**, 262107 (2011).